SCIENTIFIC REPORTS

OPEN

SUBJECT AREAS:
DRUG DISCOVERY
MOLECULAR BIOLOGY
RETINAL DISEASES

Received
23 September 2014

Accepted
8 December 2014

Published
9 January 2015

Correspondence and requests for materials should be addressed to H.T. (terasaki@med.nagoya-u.ac.jp) or H.K. (h-kaneko@med.nagoya-u.ac.jp)

Plasma-activated medium suppresses choroidal neovascularization in mice: a new therapeutic concept for age-related macular degeneration

Fuxiang Ye[1], Hiroki Kaneko[1], Yosuke Nagasaka[1], Ryo Ijima[1], Kae Nakamura[2], Masatoshi Nagaya[1], Kei Takayama[1], Hiroaki Kajiyama[2], Takeshi Senga[3], Hiromasa Tanaka[4], Masaaki Mizuno[5], Fumitaka Kikkawa[2], Masaru Hori[4] & Hiroko Terasaki[1]

[1]Department of Ophthalmology, Nagoya University Graduate School of Medicine, 65 Tsurumai-cho, Showa-ku, Nagoya 466-8550, Japan, [2]Department of Obstetrics and Gynecology, Nagoya University Graduate School of Medicine, 65 Tsurumai-cho, Showa-ku, Nagoya 466-8550, Japan, [3]Division of Cancer Biology, Nagoya University Graduate School of Medicine, 65 Tsurumai-cho, Showa-ku, Nagoya 466-8550, Japan, [4]Institute of Innovation for Future Society, Nagoya University, Furo-cho, Chikusa-ku, Nagoya 464-8603, Japan, [5]Center for Advanced Medicine and Clinical Research, Nagoya University Hospital 65 Tsurumai-cho, Showa-ku, Nagoya 466-8560.

Choroidal neovascularization (CNV) is the main pathogenesis of age-related macular degeneration (AMD), which leads to severe vision loss in many aged patients in most advanced country. CNV compromises vision via hemorrhage and retinal detachment on account of pathological neovascularization penetrating the retina. Plasma medicine represents the medical application of ionized gas "plasma" that is typically studied in the field of physical science. Here we examined the therapeutic ability of plasma-activated medium (PAM) to suppress CNV. The effect of PAM on vascularization was assessed on the basis of human retinal endothelial cell (HREC) tube formation. In mice, laser photocoagulation was performed to induce CNV (laser-CNV), followed by intravitreal injection of PAM. N-Acetylcysteine was used to examine the role of reactive oxygen species in PAM-induced CNV suppression. Fundus imaging, retinal histology examination, and electroretinography (ERG) were also performed to evaluate PAM-induced retinal toxicity. Interestingly, HREC tube formation and laser-CNV were both reduced by treatment with PAM. N-acetylcysteine only partly neutralized the PAM-induced reduction in laser-CNV. In addition, PAM injection had no effect on regular retinal vessels, nor did it show retinal toxicity *in vivo*. Our findings indicate the potential of PAM as a novel therapeutic agent for suppressing CNV.

Age-related macular degeneration (AMD) is a leading cause of blindness in most industrialized nations[1,2]. Of the 2 phenotypes of AMD, i.e., wet AMD and dry AMD, wet AMD is characterized by the invasion of choroidal neovascularization (CNV) into the sensory retina, and CNV followed by hemorrhaging in the subretinal space causes severe visual impairment[3]. The overexpressed proangiogenic cytokine vascular endothelial growth factor (VEGF) has been identified in patients with wet AMD, and anti-VEGF antibody treatment is the current standard treatment for wet-AMD[4–6]. However, repeated injections into the eyes place a heavy burden on aged patients, both physically and mentally, partially because the incidence of recurrence even after repeated (monthly) administrations is not low. Therefore, additional treatments apart from anti-VEGF therapy are desired for suppressing CNV[7,8].

Plasma medicine represents the medical application of ionized gas "plasma" that is typically studied in the field of physical science. A certain percentage of all atoms and molecules in nature exist in plasma[9]. Usually the clinical usage of plasma, via the supply of energy containing free charges, free radicals, excited molecules, and energetic photons, is related to chemical treatment or radiotherapy. The initial type of plasma in life sciences, thermal plasma, was used to sterilize surgical tools. Subsequent technical developments introduced a new generation of plasma known as nonequilibrium atmospheric pressure plasma (NEAPP), also referred to as non-thermal plasma or low-temperature plasma, and it has been challenging the advanced practical use[10]. In recent years, NEAPP therapy has been investigated as a new medical tool[11–13]. Researchers have focused on the effects of non-thermal

plasma containing reactive species on biological targets. Therapeutic trials have been performed in relation to tissue sterilization, blood coagulation, wound healing, and dental bleaching[14–16]. In addition, several studies have revealed that NEAPP induces apoptosis in several types of cancer cells[17–20].

Because angiogenesis, an important concept in cancer research, is also the main pathogenesis of wet AMD, we hypothesized that plasma-activated medium (PAM) could exert an anti-angiogenic effect on blood vessel growth in the eye. No study investigating the effects of PAM on ocular angiogenesis has been reported. Therefore, we examined the effects of PAM on the pathogenesis of CNV *in vivo* and *in vitro* to explore the therapeutic potential of PAM against AMD. The present study is the first to indicate that PAM has a potential anti-angiogenic effect on CNV in wet AMD.

Results

PAM reduced HREC tube formation. First, we examined the effect of PAM treatment on vessel tube formation *in vitro*. After 4 h of incubation with PAM, the ability of human retinal endothelial cells (HRECs) to form vascular tubes *in vitro* was clearly inhibited compared with the control ($P = 2.2 \times 10^{-9}$, Kruskal–Wallis test). The observed number of branching points showed that different concentrations of PAM (4%, 10%, and 25%) dose dependently blocked tube formation by 54% (0.46 ± 0.06, $n = 12$, $P = 1.0 \times 10^{-4}$) with 4% PAM, 81% (0.19 ± 0.02, $n = 12$, $P = 4.3 \times 10^{-5}$) with 10% PAM, and 95% (0.05 ± 0.02, $n = 12$, $P = 4.5 \times 10^{-5}$) in 25% PAM compared with the control (0% PAM) medium (1.00 ± 0.05, $n = 12$, Steel's test, Figure 1).

Intravitreal injection of PAM suppressed CNV. We examined the ability of PAM to reduce angiogenesis *in vivo*. As a representative *in vivo* ocular angiogenesis model, laser-CNV was induced in wild-type mice and different volumes of PAM (0.5, 1.0, and 2.0 μL) were intravitreally administered. The CNV volumes in the eyes injected with PAM were significantly lower than that in the control eye ($P = 0.0015$, Kruskal–Wallis test). Although there was no significant reduction in the laser-CNV volume in the 0.5 μL PAM-injected eye (0.85 ± 0.05, $P = 0.088$, $n = 11$, Steel's test) compared with the control (1.00 ± 0.05, $n = 11$), the laser-CNV volume was dose-dependently reduced by 33% in the eye injected with 1.0 μL PAM (0.67 ± 0.07, $P = 0.0035$, $n = 10$, Steel's test) and by 36% in the eye injected with 2.0 μL PAM (0.64 ± 0.08, $P = 0.0049$, $n = 9$, Steel's test) compared with that in the control eyes. (Figure 2) These results indicate that PAM has the potential to suppress ocular angiogenesis both *in vitro* and *in vivo*.

PAM induced apoptosis in cells responsible for CNV. Next, we explored the mechanism by which PAM reduced CNV. We visualized laser-CNV using terminal deoxynucleotidyl transferase-mediated dUTP nick end labeling (TUNEL) assays in sections of eyes injected with PAM or control phosphate-buffered saline (PBS; Figure 3). In the eyes injected with the control PBS, CNV occurred in the subretinal space, penetrating the retinal pigment epithelium (RPE, Figure 3D). Isolectin-B4 (iB4) staining confirmed CNV according to the presence of endothelial cells (Figure 3A). In contrast, the eyes injected with PAM exhibited much less CNV (Figure 3E and 3H), and co-staining with fluorescein isothiocyanate (FITC)–TUNEL showed that most of the endothelial cells involved in CNV were apoptotic (Figure 3F and 3G). We quantified the TUNEL-positive area and iB4-positive CNV area, and compared the percentages of the CNV area that was TUNEL-positive. The area corresponding to apoptotic cells was significantly greater in PAM-injected eyes than in PBS-injected eyes (Supplementary Figure 1). Furthermore, HRECs showed TUNEL-positivity after 4 h of PAM administration (Supplementary Figure 2). These results indicate that the reduction in CNV observed with PAM treatment was due to vascular endothelial cell apoptosis.

PAM reduced CNV independent of reactive oxygen species. Reactive oxygen species (ROS) are a key factor to explain the mechanism underlying the anti-tumor effects of PAM[19,21]. Therefore, we speculated that PAM-mediated CNV suppression is dependent on ROS generated by PAM. Following previous reports that used N-acetylcysteine (NAC) to neutralize ROS, we also examined if PAM-mediated CNV suppression is canceled by NAC (Figure 4). In our *in vivo* experiment, the CNV volume in eyes injected with PAM and/or NAC was reduced compared with that in control eyes ($P = 5.8 \times 10^{-4}$, Kruskal–Wallis test). Similar to the results shown in Figure 2, the CNV volume in eyes injected with PAM (1 μL) was 36% less than that in the control eyes (1.00 ± 0.05 vs. 0.64 ± 0.05, $n = 12$ and 10, $P = 4.4 \times 10^{-4}$, Steel's test). The CNV volume in eyes injected with

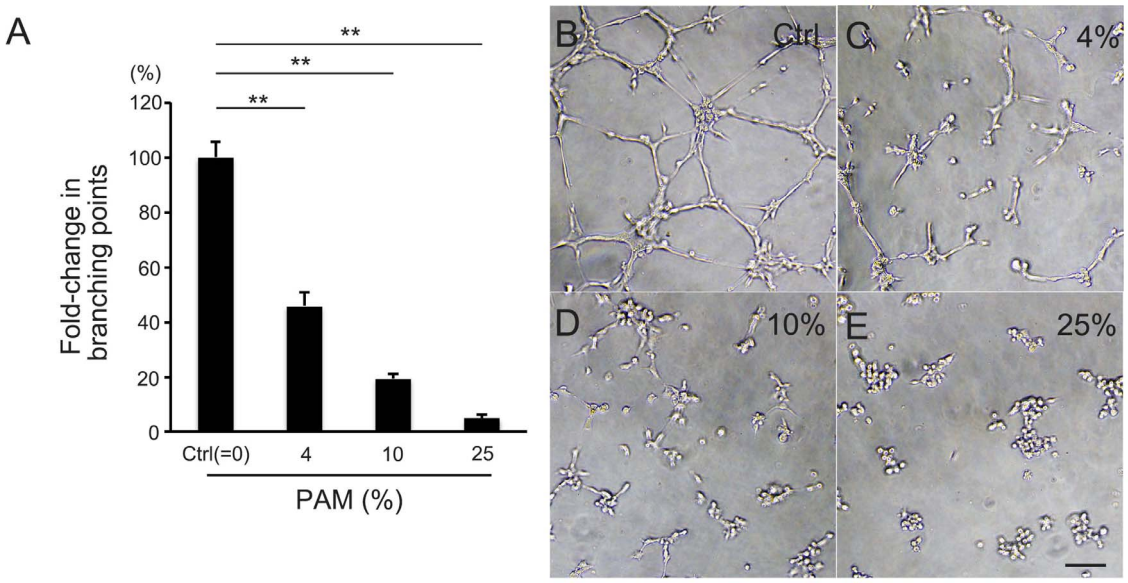

Figure 1 | PAM reduced endothelial cell tube formation *in vitro*. Tube formation of HRECs after 4 h of incubation in control EBM-2 or EBM-2-based PAM. (A) PAM was diluted at 1/25 (4%, C), 1/10 (10%, D), and 1/4 (25%, E) and compared with control (0%, B). PAM treatment reduced the number of branching points in HREC tube formation dose dependently. (B–E) Representative images of HREC tube formation. Scale bar = 100 μm. $^{**}P < 0.01$.

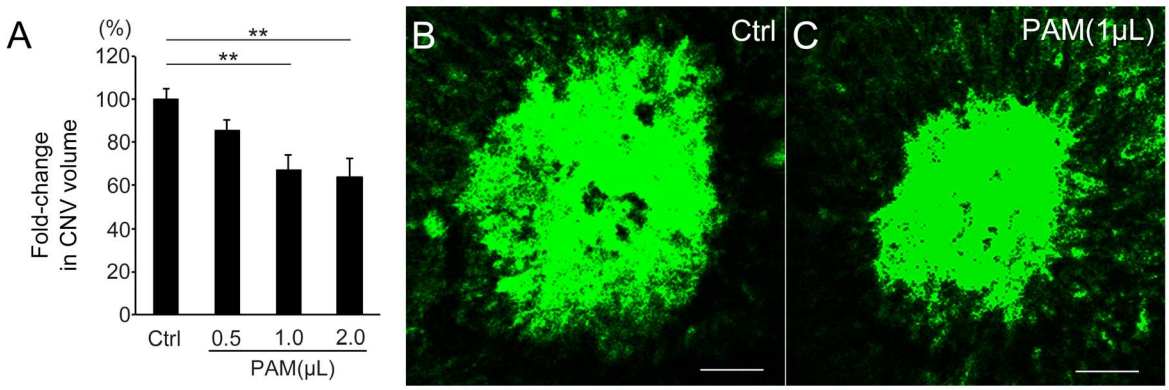

Figure 2 | PAM reduced CNV volume *in vivo*. (A) The volume of laser-CNV in 1.0 μL PAM-injected eyes was reduced by 33% ($P = 0.0035$) and 2.0 μL PAM-injected eyes was reduced by 36% ($P = 0.0049$) compared with that in control (Ctrl) eyes. (B, C) Representative images of laser-CNV in control eye (B) and 1 μL PAM-injected eyes (C). Scale bar = 50 μm, $^{**}P < 0.01$.

PAM and NAC (PAM/NAC) was also significantly less than that in the control eyes (0.83 ± 0.05, n = 13, P = 0.024, Steel's test). Although this percentage reduction in CNV volume was smaller than that obtained with injection of PAM only (Figures 2 and 4), the reduction observed after coadministration of PAM and NAC was significant. In addition, we prepared another study group and compared the laser-CNV volume in eyes injected with PAM/NAC to that in eyes injected with only NAC, and the results confirmed that PAM injection reduced CNV (Supplementary Figure 3). Taken together, these findings suggest that PAM treatment reduced CNV partly independent of ROS secretion.

PAM did not affect pre-existing retinal vessels. We examined whether PAM treatment not only inhibits neovasculature but also causes regression of pre-existing regular retinal vessels. Whole retinal flat mounts were prepared 3 days after intravitreal injections of PAM or control PBS and stained with tetramethylrhodamine isothiocyanate (TRITC)-conjugated iB4 (Figure 5). The percentages

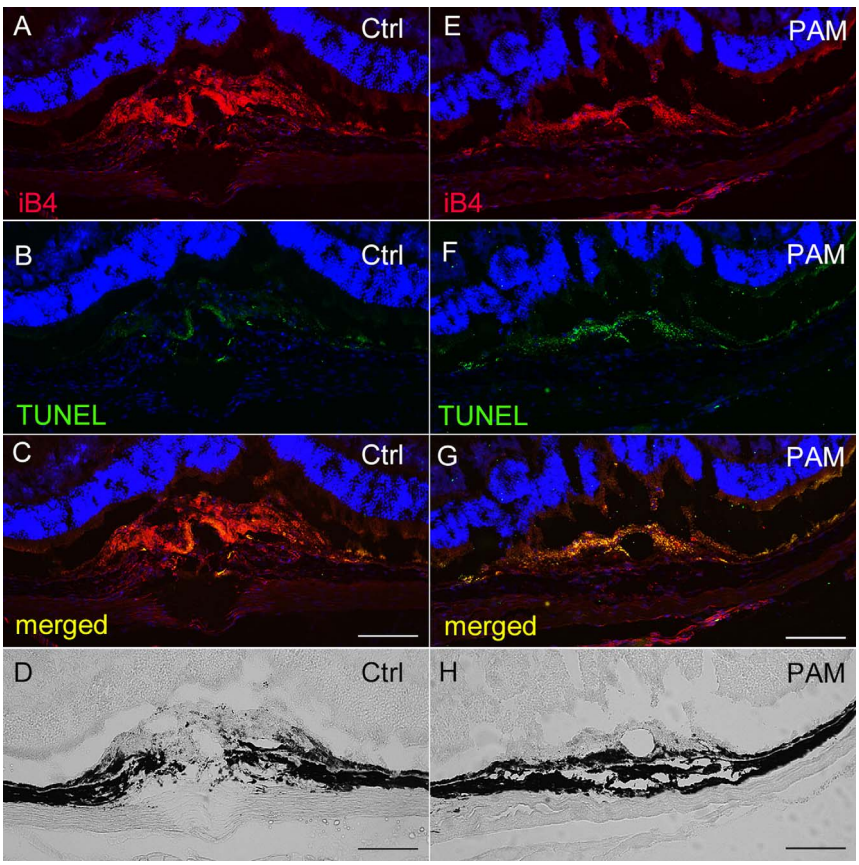

Figure 3 | PAM induced CNV apoptosis. Cryosections showing laser-CNV in eyes injected with PAM (E–H) or control (Ctrl) PBS (A–D). (A, E) TRITC-iB4 staining showed laser-CNV, which was also confirmed by phase-contrast microscopy (D, H). Images of eyes injected with PAM showed suppression of CNV (E, H) compared with that observed in control eyes (A, D). (B, F) FITC-TUNEL staining revealed apoptosis-positive cells in the laser-injured regions. (C, G) Merged images showed that eyes injected with PAM (G) showed more TUNEL-positive cells in the CNV areas than control eyes (C). Scale bar = 100 μm.

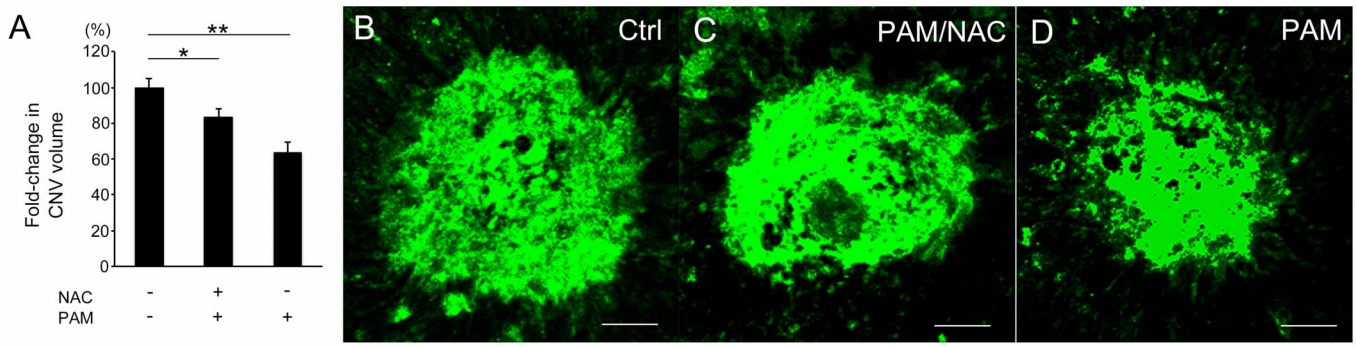

Figure 4 | NAC treatment did not completely neutralize the PAM-induced reduction in CNV. (A) The laser-CNV volume in eyes injected with both 1.0 μL PAM and NAC (presumed final concentration of 10 mM) was significantly reduced by 17% ($P = 0.024$) compared with that in eyes injected with control. (B–D) Representative images of laser-CNV in a control PBS-injected eye (B), PAM/NAC-injected eye (C), and PAM-injected eye (D). Scale bar = 50 μm, $*P < 0.05$. $**P < 0.01$.

of specific retinal regions occupied by retinal vessels did not differ significantly between eyes injected with PAM and those injected with PBS. These results indicate that PAM did not induce vessel regression among pre-existing regular retinal vessels (1.00 ± 0.06 vs. 1.12 ± 0.05, P = 0.09, n = 8; Figure 5). Therefore, we speculated that PAM selectively targets proliferating cells. To test this hypothesis, we further examined the HREC proliferation by WST-1 assay. As we expected, PAM reduced HREC proliferation dose dependently (Supplementary Figure 4).

Change in VEGF expression after PAM administration. VEGF is the main factor involved in the exacerbation of CNV in wet-AMD. It is important to know whether PAM-induced CNV suppression is related to VEGF expression. We therefore examined mouse VEGF expression in the RPE/choroid complex containing laser-CNV after PAM administration. Compared with the expression of VEGF in PBS-injected eyes, that in PAM-injected eyes was significantly reduced (Supplementary Figure 5).

PAM did not induce retinal toxicity. We also evaluated the retinal toxicity of intravitrealy injected PAM (Figure 6). Fundus imaging and retinal section analyses were applied to observe retinal degeneration. In addition, electroretinography (ERG) was used to evaluate functional changes after PAM injection on days 0 and 3. All examinations were performed 7 days after PAM injection. PAM-injected eyes did not show retinal degeneration in the fundus (n = 10). H&E-stained cryosections of PAM-injected eyes also showed no histological change. In addition, ERG showed that a-waves (photoreceptor function) and b-waves (inner retinal function) from PAM-injected eyes were not reduced compared with those in counterpart eyes injected with control medium (a-wave: 1.00 ± 0.08 vs. 1.02 ± 0.11, P = 0.85, n = 9; b-wave: 1.00 ± 0.08 vs. 0.99 ± 0.10, P = 0.97, n = 9). These results indicate that intravitreal injection of PAM reduced laser-CNV without causing retinal toxicity.

Methods

Generation of PAM. PAM was generated as described previously[19]. In brief, NEAPP with ultra-high electron density (approximately $2 \times 10^{13}/mm^3$) provided ultra-high O density, estimated to be approximately $4 \times 10^{12}/mm^3$ [22,23]. The discharge conditions for NEAPP were an argon gas atmosphere (2 standard liters/min; slm) and excitation by application of 10 kV of a 60-Hz commercial power supply to 2 electrodes separated by a distance of 8 mm[19,24]. The plasma source was placed centrally and 2 mm over 5.5 mL PBS or culture medium in a well of a 12-well plate, and the duration of plasma treatment was 600 s in all studies (Supplementary Video). The use of the same distance between the plasma source and the medium is critical for obtaining reproducible data. PAM was prepared using ultrapure PBS for *in vivo* experiments and recommended culture medium for *in vitro* experiments. In our study, the same conditions were used for all PAM preparations and for all experiments.

Animals. Male wild-type C57BL/6J mice (CLEA, Tokyo, Japan) aged 6–8 weeks were used. The mice were randomly assigned to standard cages, with 4–5 animals per cage, and kept in standard housing conditions under a 12-h light/dark cycle. For all procedures, the animals were anesthetized with intraperitoneal injection of 400 mg/kg Avertin (2.5% 2,2,2-tribromoethyl and tertiary amyl alcohol; Sigma-Aldrich, St Louis, MO, USA), and pupils were dilated with a combination of 0.5% tropicamide and 0.5% phenylephrine (Mydrin-P; Santen, Osaka, Japan). The use of animals in the experimental protocol was approved by the Nagoya University Animal Care Committee. All animal experiments were performed in accordance with the guidelines of the ARVO Statement for the Use of Animals in Ophthalmic and Vision Research.

Mouse model of laser-induced CNV (laser-CNV). Laser-CNV was generated as described previously[7]. For laser-CNV volume analysis, four spots of laser photocoagulations (532 nm laser; power, 180 mW; duration, 100 ms; diameter,

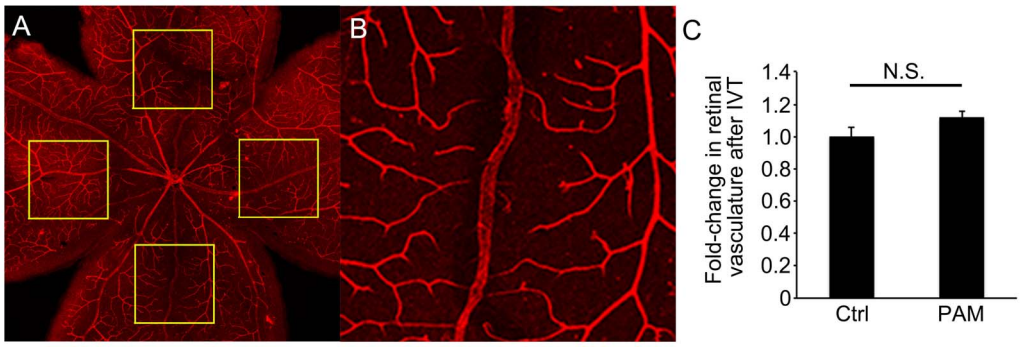

Figure 5 | PAM did not induce regression of pre-existing retinal vessels. (A) Low magnification image of a flat-mounted retina stained with TRITC-iB4 to visualize pre-existing retinal vessels. (B) High magnification image of retinal vessels in a box in (A). Each inset is 750 × 750 μm in size and 1 mm from the optic nerve. (C) The proportions of the demarcated areas occupied by retinal vessels in eyes injected with PAM were not significantly different from those in control eyes (P = 0.093, n = 8). N.S. = not significant. IVT = intravitreal injection.

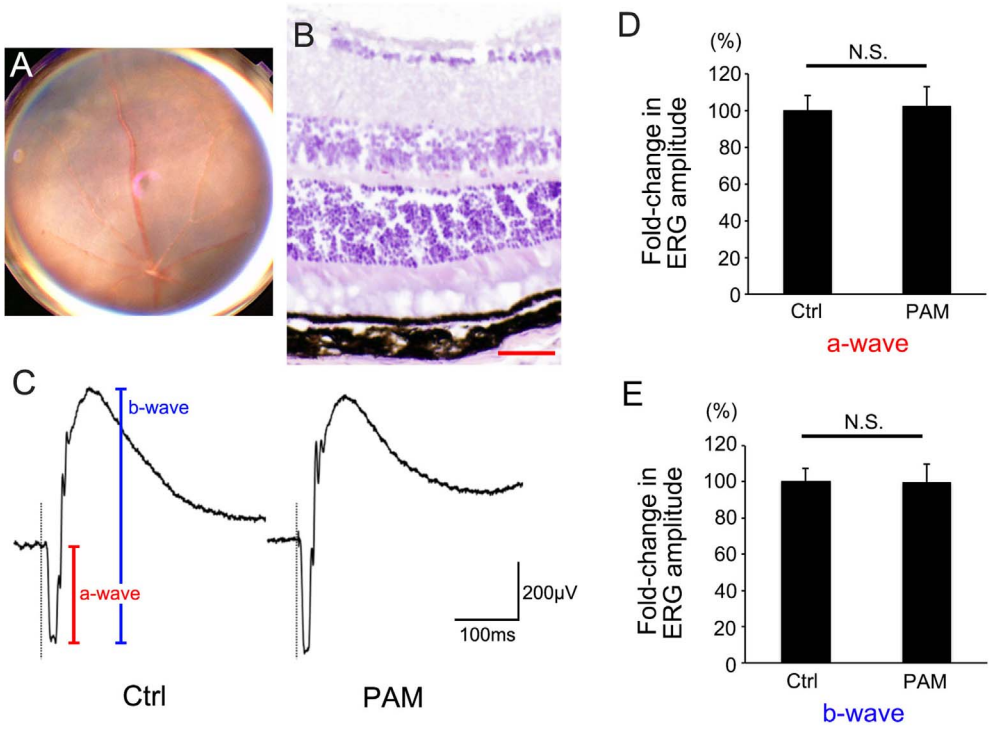

Figure 6 | PAM did not exhibit retinal toxicity. (A) Color fundus image and (B) H&E staining of a cryosection of wild-type mouse eyes injected with PAM showing no retinal degeneration. (C) Representative electroretinogram from an eye injected with PAM. (D, E) Neither ERG a-waves (D) nor b-waves (E) showed significant differences between eyes injected with PAM and control (Crtl) eyes. Scale bar (B) = 50 μm. N.S. = not significant.

75 μm; Novus Verdi; Coherent Inc., Santa Clara, CA, USA) were placed in the fundus of each eye on day 0 by an individual blinded to the group assignment, as described previously[25]. The laser spots were created around the optic nerve using a slit-lamp delivery system, and a coverslip was used as a contact lens. The morphologic end-point of the laser injury was the appearance of a cavitation bubble, which is the sign of Bruch's membrane disruption. For enzyme-linked immunosorbent assay (ELISA) analysis, 16 spots of laser photocoagulation were placed in each mouse eye.

Laser-CNV volume analysis. Laser-CNV volume was measured using a method similar to that described previously[7]. In brief, 1 week after laser injury, the eyes were enucleated and fixed with 4% paraformaldehyde (PFA). The eyecups obtained by removing the anterior segments were incubated with 0.5% FITC-conjugated iB4 (Sigma-Aldrich). CNV was visualized using a blue argon laser (488 nm wavelength) and a confocal laser scanning microscope (Eclips C1 confocal; Nikon, Tokyo, Japan). Horizontal optical sections were obtained at 1-μm intervals from the top of the CNV to the surface of the RPE. The images of each layer were stored digitally, and the area of CNV was measured using ImageJ software. The summation of the whole fluorescent area in each horizontal section was used as an index for the volume of CNV. The average volume obtained from all laser spots (3–4 spots) per eye was calculated (n = number of eyes).

Intravitreal injection of PAM and NAC. To test the effect of PAM on the pathogenesis of CNV, 0.5, 1, or 2 μL of PAM was injected immediately after the induction of laser-CNV on day 0 and on day 3. Laser-CNV in the eyes injected with each volume of PAM was compared with that in control eye. To explore the possibility of involvement of ROS in PAM-induced CNV reduction, NAC (100 mM/μL) was mixed with 1 μL PAM and co-administered intravitreally on day 0 immediately after laser-CNV induction and on day 3. First, laser-CNV in eyes injected with PAM/NAC was compared with those injected with control PBS or PAM alone. In addition, as an independent study, laser-CNV in eyes injected with PAM/NAC was compared with that in eyes injected with NAC alone.

To evaluate the retinal toxicity of PAM, PAM was injected intravitreally on day 0 and day 3, and fundus imaging, retinal histology examination, and ERG were performed on day 7. Intravitreal injection was performed with a 33-gauge needle (Ito Corporation, Shizuoka, Japan).

Retinal histology and TUNEL visualization of mouse laser-CNV and HRECs. To examine the retinal histology, the eyes were enucleated 7 days after PAM injection. For TUNEL visualization of laser-CNV after PAM treatment, the eyes were enucleated 3 days after laser photocoagulation and intravitreal injection of PAM or control PBS. Mouse eyes were enucleated and fixed in 4% PFA. Then, the eyes were prepared as eyecups, cryoprotected in 30% sucrose, embedded in an optimal cutting temperature compound (Tissue-Tek OCT; Sakura Finetek, Torrance, CA, USA), and cryosectioned into 10-μm sections. Retinal histology was confirmed with hematoxylin and eosin (H&E) staining. For TUNEL staining, the sections were stained with 30 μg/mL TRITC-conjugated iB4 (Sigma-Aldrich), an FITC-labeled reagent of the In Situ Cell Death Detection kit (Roche Diagnostics, Mannheim, Germany), and 0.3 mg/mL 4′,6-diamidino-2-phenylindole (DAPI; Invitrogen, Carlsbad, CA, USA) for 1 h. HRECs were fixed with 2% PFA for 20 minutes at room temperature, and stained using the In Situ Cell Death Detection kit (FITC-TUNEL) and DAPI after 4-h incubation of PAM. Images were taken with a BioImaging Navigator fluorescence microscope (BZ-9000; Keyence, Osaka, Japan).

ELISA. Mouse VEGF levels were measured using an enzyme-linked immunosorbent assay (ELISA) as previously described[7,26]. In brief, 3 days after laser photocoagulation and intravitreal injection of PAM or control PBS, protein lysates were prepared from the RPE/choroid complex using radioimmunoprecipitation assay buffer (Sigma-Aldrich) with a protease inhibitor cocktail (Roche Diagnostics Corporation, USA). The lysate was centrifuged at 15,000 rpm for 15 minutes at 4°C, and the supernatant was collected. Protein concentrations were determined using a Bradford assay kit (Bio-Rad, USA) with bovine serum albumin as a standard. The level of VEGF was measured with mouse VEGF ELISA kit (MMV-00, R&D Systems) according to the manufacturer's protocol. All procedures were conducted at 4°C until the final washing step was completed. The plates were analyzed by measuring the absorbance at 450 nm (reference at 570 nm) using a plate reader (Bio-Rad). Duplicate evaluations were performed for each sample.

WST-1 cell proliferation assay. Proliferative activities of HRECs were evaluated with WST-1 colorimetric assay (Roche) following manufacturer's instructions. Four-hours after treating 5×10^3 HRECs with different concentration of PAM, the plates were analyzed by measuring absorbance at 450 nm (reference at 700 nm) using a plate reader (Bio-Rad). Duplicate evaluations were performed for each sample.

Retinal flat mounting and vessel staining. Seven days after intravitreal injection of PAM, eyes were fixed with 4% PFA and stained with 10 μg/mL TRITC-conjugated iB4 as described previously[27]. After each flat-mounted retina was visualized by confocal microscopy (Eclips C1), images of four 750 × 750-μm squares located 1 mm superior, temporal, inferior, and nasal to the center of the optic nerve were analyzed using ImageJ software. The percentage of the area occupied by vessels was calculated, and the average vessel area (%) was compared between PAM-injected eyes and control eyes.

Fundus imaging. Mouse ocular fundus images were obtained using a high-resolution digital fundus camera (TRC-50DX; Topcon, Tokyo, Japan). For adjusting the focus on the mouse fundus, a 20-diopter lens was placed in contact with the fundus camera lens[28].

ERG in mice. Scotopic electroretinograms were recorded as described previously[29,30]. In brief, the animals were adapted to darkness overnight and anesthetized with intraperitoneal injection of Avertin. After dilating the pupils, electroretinograms were recorded from the corneal surface with a coiled platinum wire that made contact through a thin layer of 1% methylcellulose. A similar wire placed in the conjunctival sac and a needle electrode inserted in the tail served as the reference and ground electrodes, respectively. Electroretinograms were amplified by 1000× with a bandpass of 1–300 Hz. The ERG results were stored electronically. Strobe flash stimuli were presented in a Ganzfeld bowl. The maximum luminance was 1.0 log cd-s/m^2 (photopic units), and neutral density filters were used to reduce the full intensity of the stimulus.

Tube formation assay. To evaluate the effectiveness of PAM for preventing angiogenesis, a tube formation assay was performed, as described previously[31]. In brief, HRECs (Cell Systems; Kirkland, WA, USA) were cultured with endothelial basal medium (EBM)-2 (Lonza, Tokyo, Japan) in an incubator with 5% CO_2 in air. Extracellular matrix gels were prepared using a Chemicon *in vitro* angiogenesis assay kit (EMD Millipore, Billerica, MA). Gels were solidified in wells of a 96-well microplate, and 1.0×10^4 HRECs were added to the surface of each gel in EBM-2-based PAM or control media. After 4 h of incubation, the images of formed tubes were taken using a phase contrast microscope (FSX-100, Olympus, Tokyo, Japan). The numbers of branching points per area were calculated using ImageJ as previously described[32,33].

Statistical analysis. Results are expressed as mean ± standard error of the mean (SEM) values (n = number of samples). The result for the control sample was defined as 100%, and the percent difference relative to the control was calculated for each sample. The data from tube formation assays of HRECs treated with different concentrations of PAM and the analyses of laser-CNV volume upon injection of different volumes of PAM only, PAM and NAC, and NAC only were analyzed with the Kruskal–Wallis test, and if significance was detected ($P < 0.05$), Steel's test was applied for comparison with the control. The data from other examinations were analyzed statistically using the Mann–Whitney U test (unpaired samples). Differences were considered to be statistically significant at $P < 0.05$.

Discussion

In this study, we demonstrated that PAM reduced mouse CNV and thus has therapeutic potential for treating wet AMD. It was previously reported that proliferation, migration, and tube formation of arterial endothelial cells were enhanced upon exposure to NEAPP via ROS-induced fibroblast growth factor-2 release[34]. In addition, CNV is reported to be affected by ROS reactions[35]. However, photodynamic therapy with verteporfin is clinically approved in many countries as a treatment to suppress CNV in wet AMD[36]. In this therapy, photosensitized verteporfin generates ROS[37], which results in the regression of CNV in the fundus. Previous reports revealed that PAM suppresses tumor cell proliferation by upregulating ROS secretion in target cells, and this effect of PAM is nullified by co-administration of NAC[19,21]. These previous findings indicated the possibility that although ROS reactions have bilateral effects on angiogenesis, PAM-generated ROS can act as anti-angiogenesis factors in case of CNV. Therefore, to explore whether the PAM-induced reduction in CNV was due to ROS reactions, we examined laser-CNV with simultaneous injections of PAM and NAC, which neutralizes ROS[38,39]. Previous reports, however, have shown that NAC alone has an anti-angiogenic effect in CNV[40]. Moreover, a high concentration of NAC (>10 mg/mL) has been reported to induce retinal toxicity[41]. In our study, considering the volume of mouse vitreous cavity[42–45], we applied the maximum dose of NAC within the safe range, and this dose of NAC did not cancel PAM-induced CNV suppression *in vivo*. Whereas PAM administration suppressed CNV by 33–36%, treatment with PAM and NAC decreased CNV by only 17%. Although CNV in the eyes injected with PAM and NAC was greater than that in eyes injected with PAM alone, it was less than that observed in eyes injected with control PBS. Despite limitations in the design of the present study, these results suggest that PAM inhibits ocular angiogenesis, at least in part, via a mechanism independent of ROS activity. In this study, we used HRECs for *in vitro* assays. Ideally, to elucidate the precise mechanism of the PAM-induced anti-angionenic effect on CNV, various *in vitro* experiments using cultured choroidal endothelial cells should be performed. However, our attempts to prepare cultured choroidal endothelial cells were hampered by technical difficulties. Further studies are needed using conditions more similar to those in the generation of CNV.

The discrepancies between previous results and those of the current study with respect to the effects of NEAPP and NEAPP-activated medium on CNV may be due, in part, to the conditions under which the medium was exposed to NEAPP, including the duration of treatment, distance between the medium and NEAPP source, and the NEAPP-generating device itself. Because PAM has great therapeutic potential for use in human, further studies are needed to address several important problems. First, the precise mechanism by which PAM suppresses CNV, beyond ROS induction, must be elucidated. Second, more thorough evaluations of the retinal toxicity of PAM are needed. Clinically, the use of PAM for treating ocular conditions is relatively easier compared with its application in other tissues, because ophthalmologists can deliver specific drugs and media via topical delivery modes such as intravitreal injections. In general, it is believed that local delivery of a drug directly to the target tissue cannot induce systemic changes. However, a recent study showed that intravitrealy injected anti-VEGF drugs induced systematic changes in the body[46,47]. Although our results showed that retinal function was not altered by intravitreal injection of PAM, further assessments of the side effects of PAM administration are necessary, and the conditions for PAM treatment must be optimized to avoid side effects. Finally, a specific scale for PAM dosing is required to standardize PAM treatments.

Although extensive future research is needed to achieve the goal of clinical application of PAM and other NEAPP-based materials, preliminary research provides strong evidence that plasma medicine has great potential once all treatment conditions are appropriately optimized. For instance, higher therapeutic efficacy of anti-VEGF therapies can be expected upon combination with PAM as a solution. Toward the goal of clinical application of PAM to inhibit CNV, our study contributes proof-of-principle evidence of the therapeutic potential of PAM for use in treating ocular diseases.

1. Ambati, J. *et al.* Age-related macular degeneration: etiology, pathogenesis, and therapeutic strategies. *Surv Ophthalmol* **48**, 257–293 (2003).
2. Bird, A. C. Therapeutic targets in age-related macular disease. *J Clin Invest* **120**, 3033–3041 (2010).
3. de Jong, P. T. V. M. Mechanisms of disease: Age-related macular degeneration. *New Engl J Med* **355**, 1474–1485 (2006).
4. Brown, D. M. *et al.* Ranibizumab versus verteporfin for neovascular age-related macular degeneration. *New Engl J Med* **355**, 1432–1444 (2006).
5. Gragoudas, E. S., Adamis, A. P., Cunningham Jr, E. T., Feinsod, M. & Guyer, D. R. Pegaptanib for neovascular age-related macular degeneration. *New Engl J Med* **351**, 2805–2816 (2004).
6. Rosenfeld, P. J. *et al.* Ranibizumab for neovascular age-related macular degeneration. *New Engl J Med* **355**, 1419–1431 (2006).
7. Kaneko, H. *et al.* Histamine receptor h4 as a new therapeutic target for choroidal neovascularization in age-related macular degeneration. *Br J Pharmacol* **171**, 3754–3763 (2014).
8. Takeda, A. *et al.* CCR3 is a target for age-related macular degeneration diagnosis and therapy. *Nature* **460**, 225–230 (2009).
9. Fridman, A. *Plasma chemistry*. (Cambridge University Press, 2008).
10. Yamazaki, H. *et al.* Microbicidal activities of low frequency atmospheric pressure plasma jets on oral pathogens. *Dent Mater J* **30**, 384–391 (2011).
11. Fridman, G. *et al.* Applied plasma medicine. *Plasma Process Polym* **5**, 503–533 (2008).
12. Morfill, G., Kong, M. G. & Zimmermann, J. Focus on plasma medicine. *New J Phys* **11**, 115011 (2009).
13. Yousfi, M., Merbahi, N., Pathak, A. & Eichwald, O. Low-temperature plasmas at atmospheric pressure: toward new pharmaceutical treatments in medicine. *Fundam Clin Pharmacol* **28**, 123–135 (2014).
14. Brun, P. *et al.* Disinfection of ocular cells and tissues by atmospheric-pressure cold plasma. *PLoS One* **7**, e33245 (2012).
15. Fridman, G. *et al.* Blood coagulation and living tissue sterilization by floating-electrode dielectric barrier discharge in air. *Plasma Chem Plasma Process* **26**, 425–442 (2006).
16. Lee, H. W. *et al.* Tooth bleaching with nonthermal atmospheric pressure plasma. *J Endod* **35**, 587–591 (2009).
17. Kim, C.-H. *et al.* Induction of cell growth arrest by atmospheric non-thermal plasma in colorectal cancer cells. *J Biotechnol* **150**, 530–538 (2010).

18. Sato, T., Yokoyama, M. & Johkura, K. A key inactivation factor of HeLa cell viability by a plasma flow. *J Phys D Appl Phys* **44**, 372001 (2011).
19. Utsumi, F. *et al.* Effect of Indirect Nonequilibrium Atmospheric Pressure Plasma on Anti-Proliferative Activity against Chronic Chemo-Resistant Ovarian Cancer Cells In Vitro and In Vivo. *PLoS One* **8**, e81576 (2013).
20. Vandamme, M. *et al.* Antitumor effect of plasma treatment on U87 glioma xenografts: preliminary results. *Plasma Process Polym* **7**, 264–273 (2010).
21. Torii, K. *et al.* Effectiveness of plasma treatment on gastric cancer cells. *Gastric Cancer* **6**, DOI: 10.1007/s10120-014-0395-6 (2014).
22. Iwasaki, M. *et al.* Nonequilibrium atmospheric pressure plasma with ultrahigh electron density and high performance for glass surface cleaning. *Appl Phys Lett* **92**, 081503 (2008).
23. Jia, F. *et al.* Laser scattering diagnosis of a 60-hz non-equilibrium atmospheric pressure plasma jet. *Appl Phys Express* **4**, 026101 (2011).
24. Iseki, S. *et al.* Selective killing of ovarian cancer cells through induction of apoptosis by nonequilibrium atmospheric pressure plasma. *Appl Phys Lett* **100**, 113702–113704 (2012).
25. Tomida, D. *et al.* Suppression of choroidal neovascularization and quantitative and qualitative inhibition of VEGF and CCL2 by heparin. *Invest Ophthalmol Vis Sci* **52**, 3193–3199 (2011).
26. Nishiguchi, K. M., Kataoka, K., Kachi, S., Komeima, K. & Terasaki, H. Regulation of pathologic retinal angiogenesis in mice and inhibition of VEGF-VEGFR2 binding by soluble heparan sulfate. *PLoS One* **5**, e13493 (2010).
27. Kaneko, H., Nishiguchi, K. M., Nakamura, M., Kachi, S. & Terasaki, H. Characteristics of bone marrow-derived microglia in the normal and injured retina. *Invest Ophthalmol Vis Sci* **49**, 4162–4168 (2008).
28. Tarallo, V. *et al.* DICER1 Loss and Alu RNA Induce Age-Related Macular Degeneration via the NLRP3 Inflammasome and MyD88. *Cell* **11**, 847–859 (2012).
29. Kleinman, M. E. *et al.* Short-interfering RNAs induce retinal degeneration via TLR3 and IRF3. *Mol Ther* **20**, 101–108 (2011).
30. Miyata, K. *et al.* Reduction of oscillatory potentials and photopic negative response in patients with autosomal dominant optic atrophy with OPA1 mutations. *Invest Ophthalmol Vis Sci* **48**, 820–824 (2007).
31. Ito, T. *et al.* Girdin and its Phosphorylation Dynamically Regulate Neonatal Vascular Development and Pathological Neovascularization in the Retina. *Am J Pathol* **182**, 586–596 (2012).
32. Bid, H. K. *et al.* Anti-angiogenic activity of a small molecule STAT3 inhibitor LLL12. *PLoS One* **7**, e35513 (2012).
33. Palomero, J. *et al.* SOX11 promotes tumor angiogenesis through transcriptional regulation of PDGFA in mantle cell lymphoma. *Blood* **124**, 2235–2247 (2014).
34. Arjunan, K. P. *et al.* Non-thermal dielectric barrier discharge plasma induces angiogenesis through reactive oxygen species. *J Roy Soc Interface* **9**, 147–157 (2012).
35. Liang, F.-Q. & Godley, B. F. Oxidative stress-induced mitochondrial DNA damage in human retinal pigment epithelial cells: a possible mechanism for RPE aging and age-related macular degeneration. *Exp Eye Res* **76**, 397–403 (2003).
36. Miller, J. W. *et al.* Photodynamic therapy of experimental choroidal neovascularization using lipoprotein-delivered benzoporphyrin. *Arch Ophthalmol* **113**, 810–818 (1995).
37. Solban, N. *et al.* Targeted photodynamic therapy. *Lasers Surg Med* **38**, 522–531 (2006).
38. Oh, S. H. & Lim, S. C. A rapid and transient ROS generation by cadmium triggers apoptosis via caspase-dependent pathway in HepG2 cells and this is inhibited through *N*-acetylcysteine-mediated catalase upregulation. *Toxicol. Appl. Pharmacol* **212**, 212–223 (2006).
39. Zafarullah, M. *et al.* Molecular mechanisms of N-acetylcysteine actions. *Cell Mol Life Sci* **60**, 6–20 (2003).
40. Hara, R. *et al.* Suppression of choroidal neovascularization by N-acetyl-cysteine in mice. *Curr Eye Res* **35**, 1012–1020 (2010).
41. Lei, H. *et al.* N-acetylcysteine suppresses retinal detachment in an experimental model of proliferative vitreoretinopathy. *Am J Pathol* **177**, 132–140 (2010).
42. Lebrun-Julien, F. *et al.* ProNGF induces TNFα-dependent death of retinal ganglion cells through a p75NTR non-cell-autonomous signaling pathway. *Proc Natl Acad Sci U S A* **107**, 3817–3822 (2010).
43. Remtulla, S. & Hallett, P. A schematic eye for the mouse, and comparisons with the rat. *Vision Res* **25**, 21–31 (1985).
44. Sharma, S. *et al.* Pharmacological studies of the mouse cone electroretinogram. *Vis Neurosci* **22**, 631–636 (2005).
45. Yu, D.-Y. & Cringle, S. J. Oxygen distribution in the mouse retina. *Invest Ophthalmol Vis Sci* **47**, 1109–1112 (2006).
46. Michels, S. Is intravitreal bevacizumab (Avastin) safe? *Br J Ophthalmol* **90**, 1333–1334 (2006).
47. Simó, R. & Hernández, C. Intravitreous anti-VEGF for diabetic retinopathy: hopes and fears for a new therapeutic strategy. *Diabetologia* **51**, 1574–1580 (2008).

Acknowledgments

The authors would like to thank Seina Ito and Reona Kimoto for technical assistance. This work was supported by a Grant-in-Aid for Young Scientists (A) and a Grant-in-Aid for Challenging Exploratory Research from the Japan Society for the Promotion of Science (H.K.), the Chukyo Longevity Medical and Promotion Foundation (H.K.), the Takeda Science Foundation (H.K.), Takeda Medical Research Foundation (H.K), Yokoyama Foundation for Clinical Pharmacology (YRY1411, H.K.), and the Hori Science and Arts Foundation (F.Y.)

Author contributions

H. Kan. and F.Y. wrote the main manuscript. F.Y., H. Kan. and R.I. prepared figures. F.Y., H. Kan., Y.N., R.I., K.N. and M.N. acquired the data. K.T., H. Kaj., T.S., H. Ta., M.M., F.K., M.H. and H. Te. worked for the analysis, interpretation of data and critical revision. All authors read and approved the final manuscript.

Additional information

Supplementary information accompanies this paper at http://www.nature.com/scientificreports

Competing financial interests: The authors declare no competing financial interests.

How to cite this article: Ye, F. *et al.* Plasma-activated medium suppresses choroidal neovascularization in mice: a new therapeutic concept for age-related macular degeneration. *Sci. Rep.* **5**, 7705; DOI:10.1038/srep07705 (2015).